International Journal of Fluid Power 12 (2011) No. 1 pp. 51-58

STUDY ON PRESSURE RESPONSE OF EJECTOR VACUUM CIRCUIT

Zhonghua Guo[1], Xiaoning Li[1], Xin Li[2] and Toshiharu Kagawa[2]

[1]*Department of Mechanical Engineering, Nanjing University of Science and Technology, Xiaolingwei 200, Nanjing 210094, P.R.China*
[2]*Precision and Intelligence Laboratory, Tokyo Institute of Technology, Nagatsuta-cho 4259, Midori-ku, Yokohama 226-8503, Japan*
guozhhua@gmail.com, Xnli2008@jsmail.com.cn, li.x.ad@m.titech.ac.jp, kagawa.t.aa@m.titech.ac.jp

Abstract

In the pneumatic vacuum systems that usually consist of air powered ejector, chamber, and resistance, the pressure response of the vacuum circuit is critical to the systematic strategic planning. This paper analyzes each component of the vacuum circuit and their effects on pressure response. Firstly, a model is proposed to calculate the pressure change by using the air status equation and ejector flow-rate characteristics. For the tested ejectors with linear flow-rate characteristics, the dynamic pressure responses are a first-order system under the isothermal condition without resistance. The proposed model has been proven experimentally to be valid and it can be used in the simulation of pressure response. Secondly, the effect of resistance inserted between ejector and chamber is analyzed by combining the flow-rate characteristics of the ejector and the resistance. The further dimensionless treatment is made by introducing a new parameter G_r^* that indicates the effect of the resistance. Finally, the effects of temperature changes on pressure responses are studied on the basis of experimental data. The pressure response is faster in the non-isothermal chamber at the beginning of vacuum generation than that in isothermal chamber but it takes a long time to reach final vacuum degree.

Keywords: ejector vacuum circuit, flow-rate characteristics, pressure response

1 Introduction

Air powered ejectors are important vacuum sources in fluid power systems. They are widely used due to their advantages such as no-running parts, high durability and environmental friendliness (Majumdar, 1996). Ejectors are used in manufacturing lines, robot systems (Dorin et al., 2006; Keskeny et al., 2006; Zhang et al., 2006; Zhang et al., 2009) and in chemical plants (Chunnanond and Aohornratana, 2004; Singhal et al., 2010) or vacuum toilets (Li and Gajurel, 2001; Fane and Schlunke, 2008; Gao et al., 2010; Li et al., 2010) to transport refrigerants, particles or human excrement safely and efficiently. Figure 1 shows a typical ejector vacuum circuit that consists of ejector, vacuum valve, and vacuum pad in a material handling system. When the ejector is supplied with compressed air of pressure P_s, the air in the closed chamber of vacuum pad is entrained and P_c is below atmospheric pressure. The lift force is then generated to handle up the work-pieces. The handling operation is commonly accomplished in seconds, and the pressure response time should be calculated precisely in the generation of vacuum. Therefore, the generation of vacuum is an important step in the whole transportation task. Considering the components of ejector vacuum circuits, the generation of vacuum is dependent on, ejector flow-rate characteristics, resistance and temperature change.

The ejector flow-rate characteristics are the relationship between suction flow rate and pressure at the vacuum port. In a theoretical model the fluid mechanics inside the ejector was studied with isentropic approximation and Reynolds transport theorem (Keenan and Neumann, 1950; Huang et al., 1999), where the flow rate was calculated as a function of vacuum pressure. To be convenient and precise, the flow rate is measured as a function of pressure at the vacuum port by using flow-rate and pressure sensors (Guo et al., 2003; Zheng et al., 2005).

As above mentioned, the generation of vacuum also depends on the flow-rate characteristics of the resistances inserted between the ejector and the chamber. According to the ISO standard (ISO6358, 1989), the flow-rate characteristics of orifice-type resistances can be expressed by the elliptical flow-rate formula when the upstream pressure for testing the resistance is higher than 0.4 MPa. In vacuum, this elliptical flow-rate formula is feasible, on the basis of experi-

This manuscript was received on 26 March 2010 and was accepted after revision for publication on 10 February 2011

mental results of orifice-type resistances used in the pneumatic vacuum circuits (Han et al., 2001).

With respect to the effect of temperature change on the generation of vacuum, the works by Otic (1970) and Kagawa (1985, 2002) have shown that the heat transfer has considerable effects on dynamic characteristics of nozzle flappers and cylinders. Thus, it is also essential to investigate the effect of temperature change on the generation of vacuum in chambers of ejector circuits. The "stop method" (Kawashima et al., 2000) is used to measure the temperature in chambers.

This paper discusses the influence on pressure response from the ejector flow-rate characteristics, the resistance effect and the temperature change. Firstly, the suction flow rate is measured as a function of pressure at the vacuum port of the ejector. A model is then proposed to calculate the pressure change during the generation of vacuum by using air status equation and ejector flow-rate characteristics. Secondly, the effect of the resistance inserted between ejector and chamber is analyzed by combining flow-rate characteristics of the ejector and the resistance. The dimensionless analysis of the resistance effect is made to easily provide references for designing the vacuum circuits. Finally, the effect of heat transfer in the chamber accompanying with the pressure response are discussed on the basis of experimental data of temperature change.

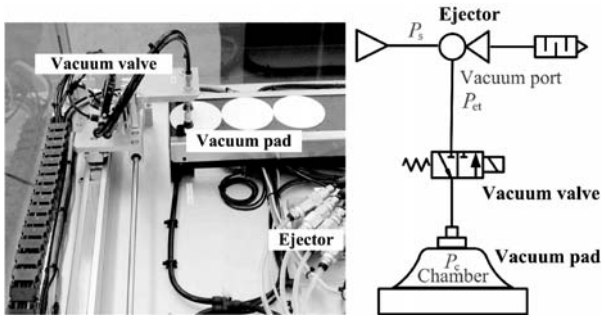

Fig. 1: *Composition of ejector vacuum circuit*

2 Ejector Flow-rate Characteristics

2.1 Air powered Ejector

The ejector is a pump-like device that uses the venturi effect of a converging-diverging nozzle to convert the pressure energy of a motive fluid to velocity energy which creates a low pressure zone that draws in and entrains a suction fluid. As shown in Fig. 2, the compressed air is used as the motive fluid at the supply port of the air powered ejector. The motive fluid is then accelerated to the speed of sound capable of entraining air at the vacuum port. The motive and entrained fluids are then mixed and discharged. As a result, the pressure at the vacuum port decreases from atmospheric pressure to vacuum. Two categories of ejectors are commonly used in fluid power systems, vacuum type and flow type. The vacuum type has higher vacuum and lower suction flow rate, while the flow type has lower vacuum and higher suction flow rate.

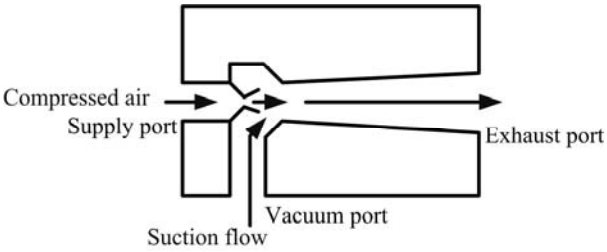

Fig. 2: *Schematics of air powered ejector*

2.2 Flow-rate Characteristics

In order to obtain the flow-rate characteristics of ejectors from experimental data, the flow rates are measured of four different ejectors bought from different companies. Four ejectors are denoted by, namely ejector 1 through 4. Ejector 1 and ejector 2 are types VCH15 and VCL15 (Pisco LTD, Japan) and ejector 3 and ejector 4 are types of CV10H and CV10L (Convum LTD, Japan). The air is supplied at a pressure of 0.5 MPa and the room temperature is 293 K. The vacuum pressure sensor is AP-10S (Keyence LTD, Japan, pressure range of -100 to 100 kPa, repeatability of ± 0.5 % of F.S.) The flow-rate sensor is a QFS-500 (Tokyo meter LTD, Japan, flow-rate range of 500 NL/min). The measured flow rates are displayed as a function of vacuum pressure at the vacuum port of the ejector in Fig. 3, where G_{et} is the suction flow rate, and P_{et} is the pressure at the vacuum port. In Fig. 3, linear fitting of the experimental data is also presented and the correlation coefficient R is 0.99. Table 1 illustrates flow-rate characteristic parameter K_{et} and b_{et} for ejectors 1 to 4.

$$G_{et} = K_{et} P_{et} - b_{et} \tag{1}$$

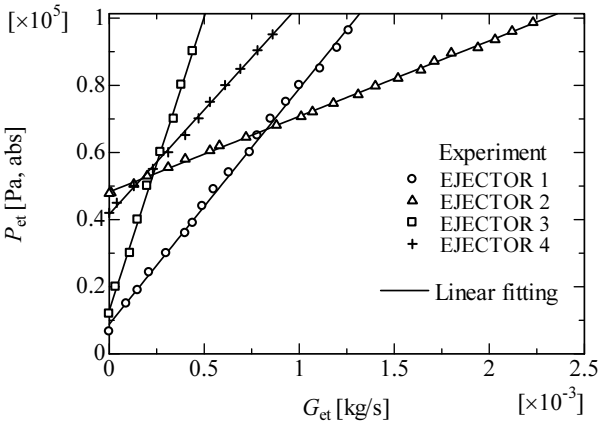

Fig. 3: *Flow-rate characteristics of ejectors*

Table 1: Flow-rate characteristics of tested ejectors

NO.	Type	K_{et} x 10^{-9} [kg/(s Pa)]	b_{et} x 10^{-4} [kg/s]
1	Vacuum	13.9	1.0
2	Flow	44.1	21.2
3	Vacuum	5.8	0.8
4	Flow	16.5	7.0

3 Pressure Response of Ejector Vacuum Circuit

3.1 Isothermal Vacuum Generation without Resistance

3.1.1 Theoretical Model

At first, the process of generating vacuum is analyzed under the isothermal condition without resistance. Once the trigger pulse opens the control valve at the supply port of the ejector, vacuum is being generated. Here, P_c is the pressure in the vacuum chamber, G_c is the suction flow rate out of chamber and V_c is the volume of the chamber. Under isothermal condition, the pressure change in the vacuum chamber is deduced from the air status equation:

$$\frac{dP_c}{dt} = \frac{G_c}{V_c} R\theta_a \tag{2}$$

Here, the flow rate out of the vacuum chamber, G_c, is equal to the suction flow rate of the ejector, G_{et}. Supposing there is no resistance at the vacuum port, the pressure, $P_{c,}$ is equal to the pressure, $P_{et.}$ By using Eq. 1 and 2, the time dependence of P_c is formulated as the following:

$$P_c = P_{et}^{\min} + e^{-\frac{t}{T_p}}(P_a - P_{et}^{\min}) \tag{3}$$

Where $P_{et}^{\min}$ is the extreme vacuum that the ejector can generate and, T_p is the pressure time constant expressed by,

$$T_p = \frac{V_c}{K_{et} R\theta_a} \tag{4}$$

The functional block diagram of the circuit is illustrated in Fig. 4. The transfer function is expressed as a first-order system:

$$F(s) = \frac{1}{1 + T_p s} \tag{5}$$

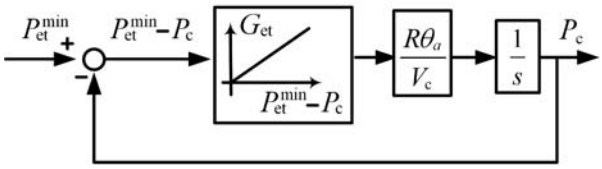

Fig. 4: *Functional block diagram under the condition of isothermal process without resistance*

3.1.2 Experimental Apparatus

Experiments are carried out to verify the theoretical deduction. It is very important to realize the isothermal condition. In the present experiments, the isothermal chamber is used to realize the isothermal condition. As shown in Fig. 5, copper wires with diameter of 0.05 mm are stuffed in a cylindrical chamber. The maximum pressure decreasing rate during the generation of vacuum is set at 100 kPa/s and the ratio of the mass of copper wires to the volume of the chamber is set at 300 kg/m^3, so that the temperature change can be controlled to be less than 3 K (Kawashima et al., 2000). As shown in Fig. 6, to study the generation of vacuum under isothermal condition without resistance, the experimental setup consists of air source, tested ejector, the control valve, vacuum chamber (isothermal), vacuum pressure sensor and A/D board, ADA16-32(CB)F (Contec, Co. Ltd. Japan). In the measurement, compressed air of pressure 0.5 MPa is supplied to the ejector.

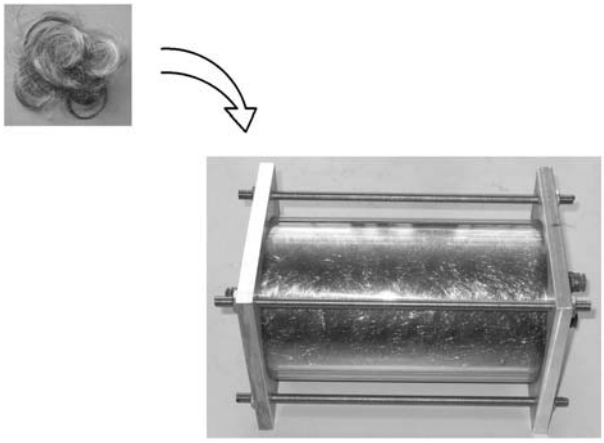

Fig. 5: *Isothermal chamber*

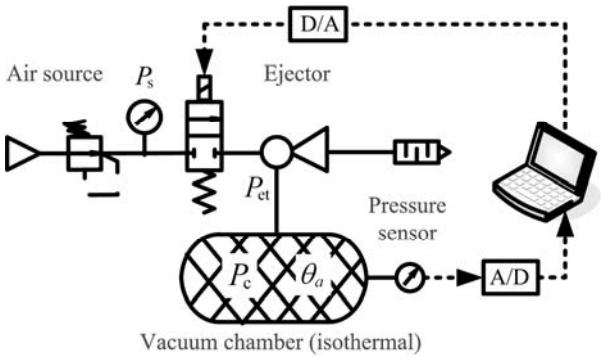

Fig. 6: *Measurement apparatus of vacuum generation under isothermal condition without resistance*

3.1.3 Results and Discussions

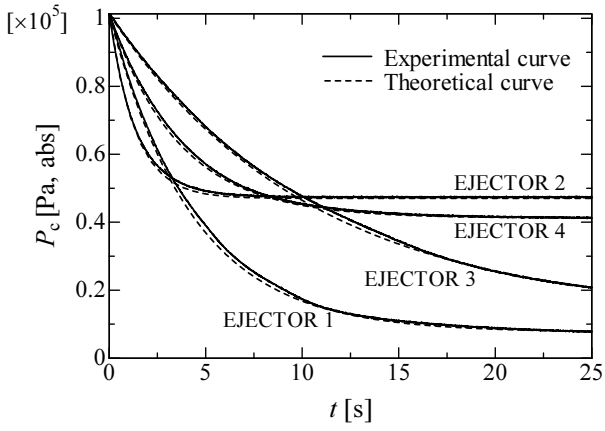

Fig. 7: *Pressure versus time during vacuum generation under isothermal condition without resistance*

The experimental data of pressure is plotted as a function of time in Fig. 7, where the pressure is recorded at the sampling time of 0.01 s by the data acquisition device. The pressure P_c can also be calculated using Eq. 3 (shown by dashed lines) as a first order pressure response. As shown in this figure, the calculation agrees well with the experimental data, suggesting that the dynamic model well simulates the generation of vacuum of the tested ejectors. Because of the existence of the resistance of the pipes that connect the ejector and chamber in the actual circuit, the responses in experiments are slower than those in simulations, and the maximum difference in the pressure is approximately 6 %.

This model can also be used to improve the efficiency of measurement on ejector flow rate by calculating the pressure change in the generation of vacuum during isothermal process. Here, in order to calculate the suction flow rate from the pressure difference, the sliding median filter is used to obtain the pressure signals. As deduced from air status equation without temperature term, the suction flow rate is calculated using Eq. 6. Considering the efficiency of measurement, it takes seconds to accomplish the generation of vacuum while it needs one hour to measure each static suction flow rate point by point.

$$G_c = \frac{V_c}{R\theta_a}\frac{dP_c}{dt} \tag{6}$$

3.2 Resistance Effect

3.2.1 Effect on Suction Flow Rate

In this section, the effect of resistance on suction flow rate is analyzed. The resistance is characterized by the sonic conductance C_r and critical pressure ratio b. The upstream pressure of the resistance is P_c and the downstream pressure of the resistance is P_{et}, as shown in Fig. 8. When the upstream pressure is P_c and the temperature is 293 K, the flow rate G_c (as a function of P_{et}) is calculated in the following two formulae:

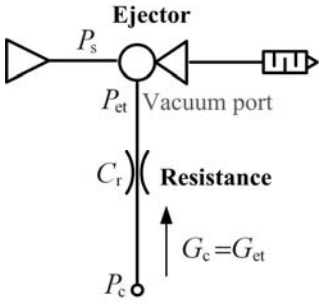

Fig. 8: *Resistance inserted between ejector and chamber*

Sonic: $$G_c = C_r \rho_0 P_c \tag{7}$$

Sub-sonic: $$G_c = C_r \rho_0 P_c \sqrt{1-\left(\frac{P_{et}/P_c - b}{1-b}\right)^2} \tag{8}$$

Together with the relation between G_{et} and P_{et} as expressed in Eq. 1, the relation between G_c and P_c is as follows:

For the condition of $C_r \le (K_{et} b)/\rho_0$,

when $$P_c < P_{et}^{min}: \quad G_c = 0 \tag{9}$$

$$P_{et}^{min} \le P_c < b_{et}/(K_{et} b - C_r \rho_0):$$

$$G_c = \left(\sqrt{\left(\frac{b_0}{2a_0}\right)^2 - \frac{c_0}{a_0}} - \frac{b_0}{2a_0}\right) P_c \tag{10}$$

$$b_{et}/(K_{et} b - C_r \rho_0) \le P_c \le P_a: \quad G_c = C_r \rho_0 P_c \tag{11}$$

For the condition of $C_r > (K_{et} b)/\rho_0$,

when $P_c < P_{et}^{min}$: $$G_c = 0 \tag{12}$$

$$P_{et}^{min} \le P_c \le P_a: G_c = \left(\sqrt{\left(\frac{b_0}{2a_0}\right)^2 - \frac{c_0}{a_0}} - \frac{b_0}{2a_0}\right) P_c \tag{13}$$

Where, P_{et}^{min} is the ejector extreme vacuum pressure, and,

$$a_0 = \left(\frac{1-b}{\rho_0 C_r}\right)^2 + \left(\frac{1}{K_{et}}\right)^2$$

$$b_0 = \frac{2}{K_{et}}\left(\frac{b_{et}/K_{et}}{P_c} - b\right)$$

$$c_0 = \frac{1}{4} K_{et}^2 b_0^2 - (b-1)^2$$

By using ejector flow-rate characteristic parameters K_{et} and b_{et} and resistance parameters C_r and b, the flow rate G_c can be calculated from P_c according to Eq. 9 to 13.

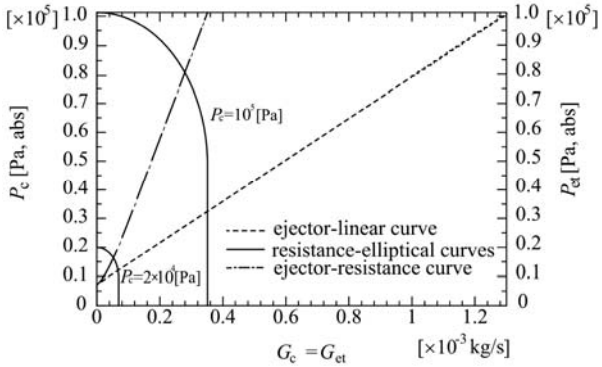

Fig. 9: *Resistance effect on flow rate*

Figure 9 shows the relationship between the flow rate and the pressure in the vacuum circuit. When the upstream pressure of the resistance is P_c, the relationship between G_c and P_{et} is characterized by resistance-elliptical curve. In the mean time, the suction flow rate G_{et} is plotted versus vacuum pressure P_{et} as ejector-linear curve according to ejector flow-rate characteristics. For the intersections of resistance-elliptical curves and ejector-linear curve, P_c is different from P_{et}. P_c is then plotted against G_c as ejec-

tor-resistance curve. The ejector-resistance curve is swerved to the direction of lower flow rate. Hence, the flow rate decreases due to the resistance effect.

3.2.2 Dimensionless Parameter G_r^*

The dimensionless resistance effect can be obtained by introducing a new parameter G_r^* which is the ratio of ejector maximum suction flow rate to resistance choked flow rate. Ejector maximum suction flow rate G_{et}^{max} is measured when the vacuum port is open to atmosphere. The resistance choked flow rate is calculated when the upstream pressure is atmospheric pressure and the flow through the resistance is choked.

$$G_r^* = \frac{G_{et}^{max}}{\rho_0 C_r P_a} \tag{14}$$

When the numerical value of G_r^* is large, the resistance has a strong influence on pressure response time. Supposing that it is under isothermal condition, the simulation on pressure response is performed by using Eq. 1 and Eq. 9 to 13, with respect to the resistance effect. Simulations are carried out using ejector 1 to 4 at different resistances. Here, because of the results of ejectors 1 to 4 exhibit the same features, only the result of ejector 1 is discussed as an example. In this simulation, resistances are installed at the vacuum port of ejector 1, where characteristic parameters G_r^* are listed in Table 2 and the volume of the vacuum chamber is 0.002 m^3. The pressure time constant T_p^0 is 1.0 s without resistance at vacuum port. When there is resistance effect, the pressure time constant T_p is larger than 1.0 s. For example, when G_r^* is 0.5, the pressure time constant is 1.08 s, 8% longer than T_p^0. By changing the value of G_r^*, the ratios of T_p to T_p^0 are illustrated in Table 2 and plotted against G_r^* in Fig. 10. As shown in Fig. 10, the ratio of T_p to T_p^0 changes slowly for relatively small G_r^*, while this ratio increases linearly for G_r^* larger than 2.0.

Table 2: Relation between G_r^* and the ratio of T_p to T_p^0

G_r^*	0	0.5	1.0	1.5	2.0	2.5	3.0	3.5	4.0	4.5	5.0
T_p / T_p^0	1.0	1.1	1.2	1.5	1.9	2.4	2.9	3.4	3.9	4.4	4.8

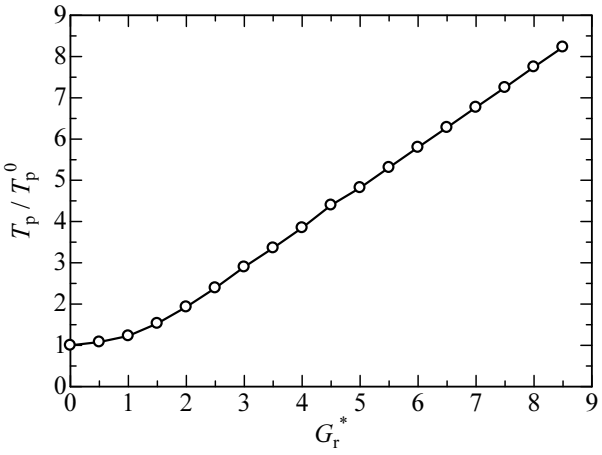

Fig. 10: *Relation between G_r^* and the ratio of T_p to T_p^0*

3.3 Effect of Temperature Change

3.3.1 Model Including Heat Transfer

During the generation of vacuum, the temperature change follows the principle of energy conservation. Pressure is calculated as a function of time using Eq. 15 and 16, where θ_c is the average temperature in the vacuum chamber, V_c is the volume of the vacuum chamber, W_c is the mass of air in the vacuum chamber, S_h is heat transfer area of the wall and h is the heat transfer ratio. Figure 11 presents a detailed functional block diagram including heat transfer.

$$\frac{dP_c}{dt} = \frac{P_c}{\theta_c}\frac{d\theta_c}{dt} + \frac{R\theta_c}{V_c} G_{et} \tag{15}$$

$$\frac{d\theta_c}{dt} = \frac{1}{c_v W_c}\left[c_p G_{et}\theta_c - c_v G_{et}\theta_c + hS_h\left(\theta_a - \theta_c\right)\right] \tag{16}$$

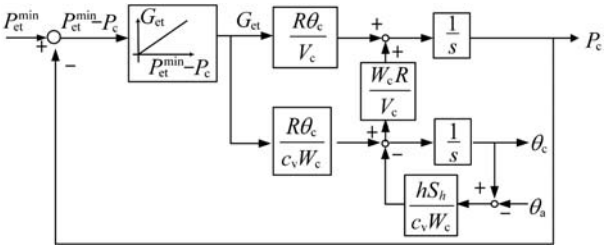

Fig. 11: *Functional block diagram including heat transfer*

3.3.2 Temperature Measurement

The influence of temperature change on the generation of vacuum is then investigated experimentally. By using the non-isothermal chamber that has the same volume as isothermal chamber, the generation of a vacuum in the non-isothermal chamber is compared with that in the isothermal chamber. Two cylindrical tanks were used for this experiment, one is made of acrylics and the other is stuffed with copper wires. The volume of the chambers is 0.005 m^3. The temperature is measured by the "stop method" (Kawashima et al., 2000). The process of the generation of vacuum is stopped at time *t*' and the pressure at that time is measured. When the temperature goes back to room temperature, the pressure is measured again. By using the two pressures and room temperature, the temperature at time *t*' can be calculated by using the Law of Charles. Change the time *t*', and temperature is plotted versus time.

Figure 12 shows the experimental result. Ejector 1 is used in this experiment. The dash line is the pressure response curve in the isothermal chamber while the solid one is that in the non-isothermal chamber. Under the isothermal condition, the pressure response is a first-order system. In the non-isothermal chamber, however, the heat transfer ratio and heat transfer area is much smaller, the pressure response is faster at the beginning of the generation of vacuum but it takes a long time for temperature recovery, and a relatively long time to reach the final vacuum degree. Considering the temperature change, when the vacuum is being generated, a large amount of air is entrained from the vacuum chamber to the ejector, with a sharp decrease in

the temperature of air inside the non-isothermal chamber. Meanwhile, the pressure response is fast in the non-isothermal chamber. After that, the temperature has a slow recovery through heat transfer, and it takes a long time to reach the final vacuum degree.

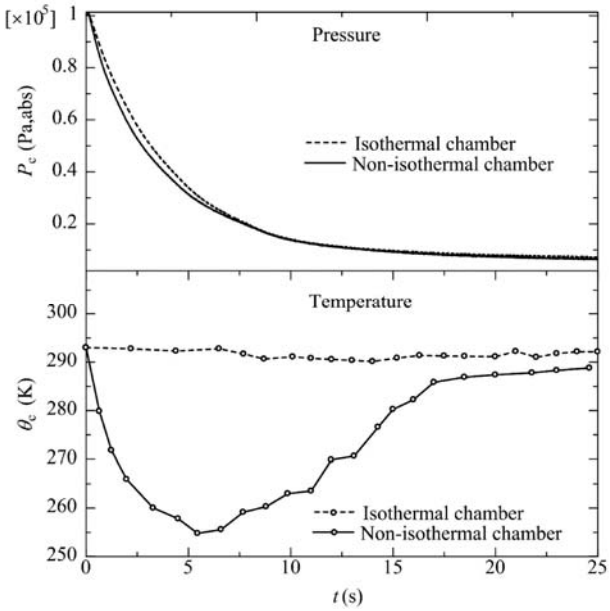

Fig. 12: *Comparison between isothermal chamber and non-isothermal chamber*

3.3.3 Effects on Different Ejectors

To discuss the effect of temperature change on the generation of vacuum of different ejectors, the experiments are performed on the same vacuum chamber using ejector 1 and 2, where the suction flow rate of ejector 2 is higher than that of ejector 1. The pressure is plotted against time for ejector 1 and ejector 2 in Fig. 13 to 14. The dimensionless pressure and time are calculated using Eq. 17 and 18.

$$P_c^* = \frac{P_c - P_{et}^{min}}{P_a - P_{et}^{min}} \tag{17}$$

$$t^* = \frac{t}{T_p} \tag{18}$$

As shown in Fig. 13 and 14, there are differences between response processes in the non-isothermal chambers of ejector 1 and 2, and the response of ejector 2 is faster than that of ejector 1. This can be evaluated by the ratio of pressure time constant to heat time constant, as deduced from Eq. 19. The first term on the right side of Eq. 19 is reduced to a constant. The other term is determined by the heat transfer ratio, heat transfer area and ejector flow-rate characteristic parameter K_{et}. Since the vacuum chamber is the same, this ratio is larger for ejector 1 compared to ejector 2 and, hence the heat transfer is more sufficient and the pressure response is closer to isothermal process. Similarly, the same experiments are carried out with ejector 3 and 4, and the response of ejector 4 is faster than that of ejector 3.

$$\frac{T_p}{T_h} = \frac{1}{\rho_0 c_v R \theta_a}\left(\frac{hS_h}{K_{et}}\right) \tag{19}$$

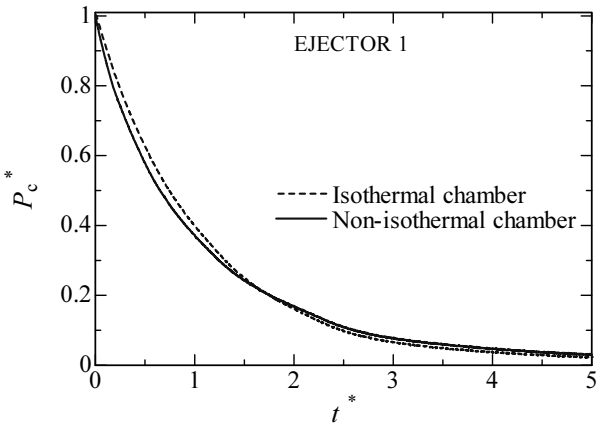

Fig. 13: *Dimensionless pressure response of ejector 1*

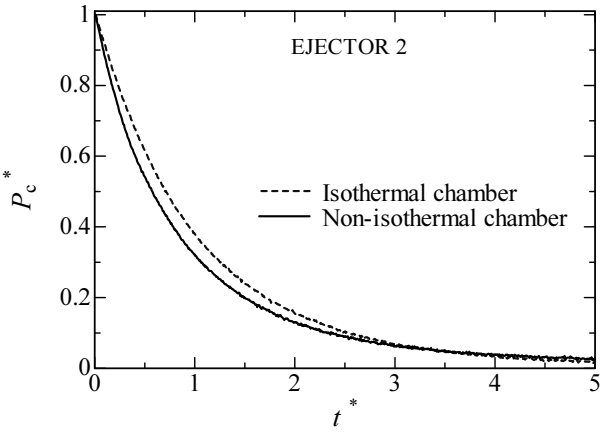

Fig. 14: *Dimensionless pressure response of ejector 2*

4 Conclusion

The model is proposed to calculate the pressure change in the generation of vacuum by using air status equation and static flow-rate characteristics of ejectors and has been proven to be effective. For the tested ejectors with linear flow-rate characteristics, the pressure responses are first-order systems under isothermal condition without resistance. The proposed model has also been used in the simulation of pressure response and improvement for measuring ejector suction flow rate by the analysis of the pressure change under isothermal conditions.

The effect of resistance inserted between the ejector and the chamber is analyzed by combining the flow-rate characteristics of ejector and resistance. The dimensionless treatment of the resistance effect is employed with new parameter G_r^* that is the ratio of ejector maximum suction flow rate to resistance choked flow rate. It is found that when G_r^* is larger, the resistance has a stronger influence on pressure response time. Therefore, when a pneumatic ejector system is designed, it must be verified that ejector flow-rate characteristics are compatible with resistance and the parameter G_r^* is small.

The effects of heat transfer on pressure responses are discussed on the basis of experimental data. The

experimental result shows that the pressure response is faster in the non-isothermal chamber at the beginning of the generation of vacuum than that in the isothermal chamber but it takes a long time to reach final vacuum degree. It is also derived from the experimental data that the pressure response is faster when the ejector flow-rate characteristic parameter K_{et} is larger.

Nomenclature

b	critical pressure ratio	[−]
b_{et}	flow-rate characteristic parameter	[kg/s]
c_p	specific heat at constant pressure	[J/(kg·K)]
c_v	specific heat at constant volume	[J/(kg·K)]
C_r	sonic conductance of resistance	[m⁴·s/kg]
G_c	mass flow rate out of vacuum chamber	[kg/s]
G_{et}^{max}	ejector maximum suction flow rate	[kg/s]
h	heat transfer ratio	[W/(m²·K)]
K_{et}	flow-rate characteristic parameter	[kg/(s·Pa)]
P_a	atmospheric pressure	[Pa,abs]
P_c	pressure in vacuum chamber	[Pa,abs]
P_s	supply pressure	[Pa,abs]
P_{et}^{min}	extreme vacuum of ejector	[Pa,abs]
R	gas constant	[J/(kg·K)]
s	Laplace variable	[1/s]
S_h	heat transfer area	[m²]
t	time	[s]
T_h	thermal time constant	[s]
T_p	pressure time constant	[s]
T_p^0	pressure time constant without resistance	[s]
V_c	volume of vacuum chamber	[m³]
W_c	air mass in vacuum chamber	[kg]
ρ_0	air density under normal conditions	[kg/m³]
θ_a	atmospheric temperature	[K]
θ_c	temperature in vacuum chamber	[K]

Acknowledgement

The authors acknowledge the financial support by China Scholarship Council and Japan Fluid Power System Society. Mr. Morozumi and Mr. Koga (PISCO LTD, Japan) are acknowledged for kind help and discussions.

Reference

Chunnanond, K. and **Aphornratana, S.** 2004. Ejectors: Applications in Refrigeration Technology. *Renewable and Sustainable Energy Reviews*, Vol. 8(2), pp. 129 - 155.

Dorin, P., **Sorin, V.**, **Adrian, M.**, **Florin, M.** and **Livia, P.** 2006. Telematics Applications for a Body Feed-positioning Station. *Proceedings of the 6th WSEAS International Conference on Distance Learning and Web Engineering*, Lisbon, Portugal, pp. 38 - 43.

Fane, S. and **Schlunke, A.** 2008. Opportunities for More Efficient Toilets in Australia -How Low Can We Go? *3rd National Water Efficiency Conference*, pp. 1 - 10.

Gao, F., **Zhou, J. X.** and **Li, M.** 2010. Numerical Simulation of Performance of Air-jet Vacuum Pump for Coach Toilet. *Zhenkong*, Vol. 47(5), pp. 63 - 67. (In Chinese)

Guo, W. Q., **Pu, R. P.** and **Han X. J.** et al. 2003. The analysis research of the aspirating mechanism and function of vacuum generator. *Zhenkong*, Vol. 40(6), pp. 54 - 56. (In Chinese)

Han, B. J., **Fujita, T.**, **Kawashima, K.** and **Kagawa, T.** 2001. Influence of Pressure Condition Change on the Flow-rate characteristics of Pneumatic Valve. *Journal of the Japan Hydraulics and Pneumatics Society*, Vol. 32(6), pp. 143 - 149

Huang, B. J., **Chang, J. M.**, **Wang, C. P.** and **Petrenko, V. A.** 1999. A 1-D Analysis of Ejector Performance. *International Journal of Refrigeration*, Vol. 22(5), pp. 354 - 364.

ISO6358. 1989. Pneumatic Fluid Power-Components Using Compressible Fluids-Determination of Flow-rate Characteristics.

Kagawa, T. 1985. Heat Transfer Effects on the Frequency Response of a Pneumatic Nozzle Flapper. *ASME. Journal of Dynamic Systems, Measurement, and Control*, Vol. 107, pp. 332 - 336.

Kagawa, T. 2002. Influence of Air Temperature Change on Equilibrium Velocity of Pneumatic Cylinder. *ASME. Journal of Dynamic Systems, Measurement and Control,* Vol. 124, 336 - 341.

Kawashima, K., **Kagawa, T.** and **Fujita, T.** 2000. Instantaneous Flow Rate Measurement of Ideal Gases. *ASME. Journal of Dynamic System, Measurement and Control*, Vol. 122(1). pp. 174 - 178.

Keenan, J. H. and **Neumann, E. P**. 1950. An Investigation of Ejector Design by Analysis and Experiment. *Journal of Applied Mechanics*, Vol. 17, pp. 299 - 305.

Keskeny, J., **Huba, A.** and **Muka, I.** 2006. High Elastic Bionic Based Robot and Gripper. *3rd International Conference on Mechatronics*, pp. 236 - 241.

Li, M., **Zhou, J.** and **Gao, F.** 2010. Modeling Study on Outdoor Vacuum Sewage System. *Zhenkong*, Vol.47 (5), pp. 66 - 70. (In Chinese)

Li, Z. and **Gajurel, D. R.** 2001. Development of Source Control Sanitation Systems in Germany. *Conference on Ecological sanitation*, pp. 1 - 4.

Majumdar, S. R. 1996. *Pneumatic systems: principles and maintenance.* McGraw-Hill Publishing Company LTD.

Otis, D. R. 1970. Thermal Damping in Gas-Filled Composite Material during Impact Loading. *ASME. Journal of Applied Mechanics,* Vol.37. pp. 38 - 43.

Singhal, G., **Tyagi, R. K.**, **Dawar, A. L.** and **Subbarao, P. M. V.** 2010. Pressure Recovery Studies

on a Supersonic Coil with Central Ejector Configuration. *Optics & Laser Technology*, Vol. 42, pp. 1145 - 1153.

Zhang, H., **Zhang, J.**, **Zong, G.**, **Wang, W.**, and **Liu, R.** 2006. "Sky Cleaner 3-A Real Pneumatic Climbing Robot for Glass-Wall Cleaning" *IEEE Robotic & Automation Magazine*, Vol. 13(1), pp. 32 - 41.

Zhang, H., **Wang, W.** and **Zhang, J.** 2009. A Novel Passive Adhesion Principle and Application for an Inspired Climbing Caterpillar Robot. *IEEE International Conference on Mechatronics*, pp. 1 - 6.

Zheng, X. R., **Zhang X.** and **Zhao Z. F.** et al. 2005. Relationship Between Structure Parameter and Performance Parameter of Vacuum Ejector. *Zhenkong*, Vol. 42(5), pp. 13 - 16. (In Chinese)

Zhonghua GUO
Born in August 1983. Ph. D applicant of Nanjing University of Science and Technology (P.R. China). She is doing research as a visiting associate in the Precision and Intelligence Laboratory of Tokyo Institute of Technology (Japan). Her Ph. D research field is pneumatic ejector system design and measurement.

Xiaoning LI
Born in February 1957. Received his Ph. D degree from Harbin Institute of Technology (P.R. China) in 1989. He is working as a professor in School of Mechanical Engineering of Nanjing University of Science and Technology. His primary research interests are modelling, simulation and control for advanced manufacturing system and pneumatic control technology.

Xin LI
Born in September 1979. Received his Ph. D degree from Tokyo Institute of Technology (Japan) in 2009. He is working as assistant professor in the Precision and Intelligence Laboratory of the institute. His primary research fields are pneumatic handling device and compressible fluid control & measurement.

Toshiharu KAGAWA
Born in November 1950. Received his M. Se and Ph. D degree from Tokyo Institute of Technology in Japan. He is working as a professor at the Precision and Intelligence Laboratory of the institute. His primary research interests are fluid dynamics, fluid measurement and control.